

PACS: 87.14.Cc, 87.16.Dg

NOVEL FLUORESCENT NEAR-INFRARED AGENT FOR BIOMEDICAL APPLICATIONS

V. Trusova¹, G. Gorbenko¹, T. Deligeorgiev², N. Gadjev²

¹*Department of Nuclear and Medical Physics, V.N. Karazin Kharkov National University
4 Svobody Sq., Kharkov, 61022, Ukraine*

²*Department of Applied Organic Chemistry, Faculty of Chemistry, University of Sofia
1164 Sofia, Bulgaria*

e-mail: valeriya.m.trusova@gmail.com

Received September 26, 2016

Squaraines represent a class of organic dyes operating in red and near-infrared regions. Due to their unique optical characteristics, such as high extinction coefficients, reduced background fluorescence and light scattering, photostability, these fluorophores attract ever-growing attention as prospective bioimaging agents. The present contribution overviews the spectral properties and some biological applications of the novel squaraine dye SQ-1. This probe was found to possess very high lipid-associating ability manifesting itself in a sharp increase of its emission. Binding of SQ-1 to the lipid bilayers containing zwitterionic and anionic lipids was found to be controlled mainly by hydrophobic interactions. Analysis of SQ-1 spectral behavior in the model membrane systems containing heme proteins revealed the dye sensitivity to the reactive oxygen species. This effect was supposed to originate from the reaction between lipid radicals and SQ-1 occurring at the squaric moiety or in its vicinity. Resonance energy transfer studies highlight the applicability of SQ-1 to structural characterization of amyloid fibrils.

KEYWORDS: squarylium dye, membrane, partitioning coefficient, lipid peroxidation, amyloid fibrils

НОВИЙ ДОВГОХВИЛЬОВИЙ ФЛОУРЕСЦЕНТНИЙ ЗОНД ДЛЯ БІОМЕДИЧНИХ ДОСЛІДЖЕНЬ

В. Трусова¹, Г. Горбенко¹, Т. Делігеоргієв², Н. Гаджев²

¹*Кафедра ядерної та медичної фізики, Харківський національний університет ім. В.Н. Каразіна
м. Свободи 4, Харків, 61022, Україна*

²*Кафедра прикладної органічної хімії, Університет Софії
1164 Софія, Болгарія*

Сквараїни представляють собою клас органічних барвників, функціонально активних у червоній та ближній інфрачервоній областях. Завдяки їх унікальним оптичним характеристикам, зокрема, високому коефіцієнту екстинкції, низькому фоновому сигналу, високій фотостабільності, ці флуорофори привертають увагу як перспективні агенти для візуалізації біомолекул. У даній роботі охарактеризовані спектральні властивості та деякі аспекти біологічного використання нового сквараїнового зонду SQ-1. Виявлено, що даний зонд має високу ліпід-асоціюючу здатність, що виражається у значному зростанні інтенсивності флуоресценції. Показано, що асоціація SQ-1 із ліпідними бішарами, що містять цвїттерійонні та аніонні ліпіди, контролюється гідрофобними взаємодіями. Аналіз спектральної поведінки SQ-1 у модельних мембранних системах, що містили гемові білки, показав, що зонд чутливий до реактивних форм кисню. В основі цього ефекту лежить, згодом, взаємодія радикалів ліпідів із зондом, що супроводжується дестабілізацією сквараїнового мостика. Дослідження індуктивно-резонансного переносу енергії виявило можливість використання SQ-1 для структурної характеристики амїлоїдних фібрил.

КЛЮЧОВІ СЛОВА: сквараїновий барвник, мембрани, коефіцієнт розподілу, перекисне окислення ліпідів, амїлоїдні фібрили

НОВЫЙ ДЛИННОВОЛНОВОЙ ФЛОУРЕСЦЕНТНЫЙ ЗОНД ДЛЯ БИОМЕДИЦИНСКИХ ИССЛЕДОВАНИЙ

В. Трусова¹, Г. Горбенко¹, Т. Делігеоргієв², Н. Гаджев²

¹*Кафедра ядерной и медицинской физики, Харьковский национальный университет им. В.Н. Каразина
пл. Свободы 4, Харьков, 61022, Украина*

²*Кафедра прикладной органической химии, Университет Софии
1164 София, Болгария*

Сквараины представляют собой класс органических красителей, функционально активных в красной и ближней инфракрасной областях. Благодаря их уникальным оптическим характеристикам, в частности, высокому коэффициенту экстинкции, низкому фоновому сигналу, высокой фотостабильности, эти флуорофоры привлекают внимание как перспективные агенты для визуализации биомолекул. В данной работе охарактеризованы спектральные свойства и некоторые аспекты биологического применения нового сквараинового зонда SQ-1. Выведено, что данный зонд обладает высокой липид-связывающей способностью, что выражается в значительном увеличении интенсивности флуоресценции. Обнаружено, что ассоциация SQ-1 с липидными бислоями, состоящими из цвїттерійонных и анионных липидов, контролируется гидрофобными взаимодействиями. Анализ спектрального поведения SQ-1 в модельных мембранных системах, содержащих гемовые белки, показал, что зонд чувствителен к реактивным формам кислорода. В основе этого эффекта лежит, предположительно, взаимодействие радикалов липидов с зондом, что сопровождается дестабилизацией сквараинового мостика. Исследование индуктивно-резонансного переноса энергии выявило принципиальную возможность применения SQ-1 для структурной характеристики амїлоїдних фибрилл.

КЛЮЧЕВЫЕ СЛОВА: сквараиновый зонд, мембрани, коэффициент распределения, перекисное окисление липидов, амїлоїдные фибриллы

The past decades have seen a renaissance of fluorescence-based approaches and methodologies reflected in the expansion of fluorescence application not only in biophysics and biochemistry, but also in medical diagnostics and treatment, flow cytometry, biotechnology, genetics, etc. [1-4]. The widespread use of fluorescence spectroscopy as a powerful analytical tool is determined by its high sensitivity, resolution, selectivity, noninvasiveness, relative simplicity and rapidity of implementation. A good deal of fluorescent reporter molecules with different spectral characteristics and designed for various purposes are available up to date [5-8]. Among a broad selection of existing fluorophores, one of the leading places belongs to the bright family of squaraine probes [9-11]. Squaraines represent the 1,3-disubstituted derivatives of squaric acid with a general donor- π -acceptor- π -donor configuration distinguished by a planar rigid geometry containing electron-withdrawing central moiety and two electron-donating groups [12]. Such a structure ensures the advantageous optical and physicochemical properties of squaraine fluorophores, including sharp and intense absorption in the red visible region (>600 nm), reduced background signal, high extinction coefficients and quantum yield, photo- and chemical stability, to name only a few. Due to their attractive absorption and fluorescence characteristics, squaraine probes have proved their versatility in a wide range of applications. Specifically, these compounds were used as prospective semi- and photoconducting materials in optical recording media, organic solar cells, xenography, nonlinear optics [13,14]. Furthermore, squaraines were employed as colorimetric sensors for detection of metal ions, such as Ca^{2+} , Mg^{2+} , Pd^{2+} , Hg^{2+} , Ag^+ , where these mesoionic dyes serve as π -donor ligands [15,16]. In addition, squaraine dyes are thought to represent the second generation of photosensitizers for photodynamic therapy [17]. Accordingly, clinical investigations showed that squaraines are nontoxic in dark but exhibit high photodynamic potential against tumor cells when exposed to light. Finally, squaraines turned out to be extremely promising in biomedical imaging since they absorb and emit in so-called optical window where the majority of biomolecules are spectroscopically inactive. Squaraines were recruited as covalent and noncovalent proteins markers [18], reporter molecules for tracing the membrane-related processes [19,20], or fluorescent probes for two- and multiphoton fluorescence bioimaging in *ex vivo* and *in vitro* studies [21]. The present work is intended to expand the application of squaraine dyes as biomolecule sensors. Specifically, in this contribution, which represents the quintessence of our previous studies [22-24], we highlight some interesting features of the novel squaraine fluorophore SQ-1, concerning its i) lipid-associating behavior; ii) potential in biosensing area, particularly, in free radical detection; iii) informativeness in structural characterization of amyloid fibrils.

MATERIALS AND METHODS

Materials

Squaraine dye SQ-1 and its structural analog, the polymethine dye V2, having the same end groups as SQ-1, but lacking the central squaric moiety, were synthesized at the Faculty of Chemistry, University of Sofia [22]. Egg yolk phosphatidylcholine (PC), phosphatidylglycerol (PG) and beef heart cardiolipin (CL) were purchased from Avanti Polar Lipids (Alabaster, AL). Chicken egg white lysozyme was from Sigma (St. Louis, MO, USA). Horse heart cytochrome *c* (ferric form) was from Fluka (Buchs, Switzerland). Horse blood methemoglobin, thiourea (TM) and butylated hydroxytoluene (BHT) were purchased from Reanal (Hungary). Iron sulfate (FeSO_4) and ascorbate were from Sigma Aldrich (Germany). All other chemicals were of analytical grade and used without further purification.

Preparation of lipid vesicles

Unilamellar lipid vesicles composed of neat PC and its mixtures with CL or PG were prepared by the extrusion method [25]. Appropriate amounts of lipid stock solutions were mixed in ethanol, evaporated to dryness under a gentle nitrogen stream, and then left under reduced pressure for 1.5 h to remove any residual solvent. The obtained thin lipid films were hydrated with 1.2 ml of 5 mM NaP_i buffer (pH 7.4) at room temperature. Thereafter lipid suspensions were extruded through a 100 nm pore size polycarbonate filter (Nucleopore, Pleasanton, CA). The phospholipid concentration was determined according to the procedure of Bartlett [26].

Preparation of lysozyme fibrils

The reaction of lysozyme fibrillization was initiated using the approach developed by Holley and coworkers [27]. Protein solutions (3mg/ml) were prepared by dissolving lysozyme in deionized water with subsequent slow addition of ethanol to a final concentration 80%. Next, the samples were subjected to constant agitation at ambient temperature. This resulted in the formation of lysozyme fibrils over a time course of about 30 days. The amyloid nature of fibrillar aggregates was confirmed in Thioflavin T assay.

Fluorescence measurements

Steady-state fluorescence spectra were recorded with LS-55 spectrofluorimeter equipped with a magnetically stirred, thermostated cuvette holder (Perkin-Elmer Ltd., Beaconsfield, UK). Fluorescence measurements were performed at 20°C using 10 mm path-length quartz cuvettes.

The quantum yield of SQ-1 (Q_{SQ-1}) was estimated using Cy5 as a standard ($Q_{Cy5}=0.28$ [28]) according to the relationship:

$$Q_{SQ-1} = \frac{Q_{Cy5} (1 - 10^{-A_{Cy5}}) S_{SQ-1}}{(1 - 10^{-A_{SQ-1}}) S_{Cy5}}, \quad (1)$$

where A_{Cy5} and A_{SQ-1} stand for the absorbances of Cy5 and SQ-1, respectively, at the excitation wavelength; S_{Cy5} and S_{SQ-1} are the integrated areas of fluorescence spectra of Cy5 and SQ-1, respectively.

Quantum chemical calculations

Quantum chemical calculations were made using Win-Gamess software with the 6-31G(d,p) basis set, in the framework of density functional theory (DFT) and B3LYP functional. For optimization of SQ-1 ground state geometry semiempirical AM1 method with added polarization (1) and diffuse (1) functions on heavy atoms, and a polarization function on hydrogen atoms was used. All calculations were performed in gas phase.

RESULTS AND DISCUSSION

Optical properties of SQ-1 and quantum chemical calculations

SQ-1 is characterized by symmetric zwitterionic structure with central squarate bridge and two butyl tails connected to the heterocyclic chromophore moieties. Electronic symmetry of this dye results in intense and sharp absorption spectrum with a dominant maximum at 662 nm and a shoulder around 614 nm (Fig. 1, A). SQ-1 was found to be nearly non-fluorescent in aqueous media but exhibit intense emission in ethanolic solutions, centered at 683 nm (Fig. 1, B). Notably, the Stokes shift of SQ-1 is relatively small (*ca.* 21 nm).

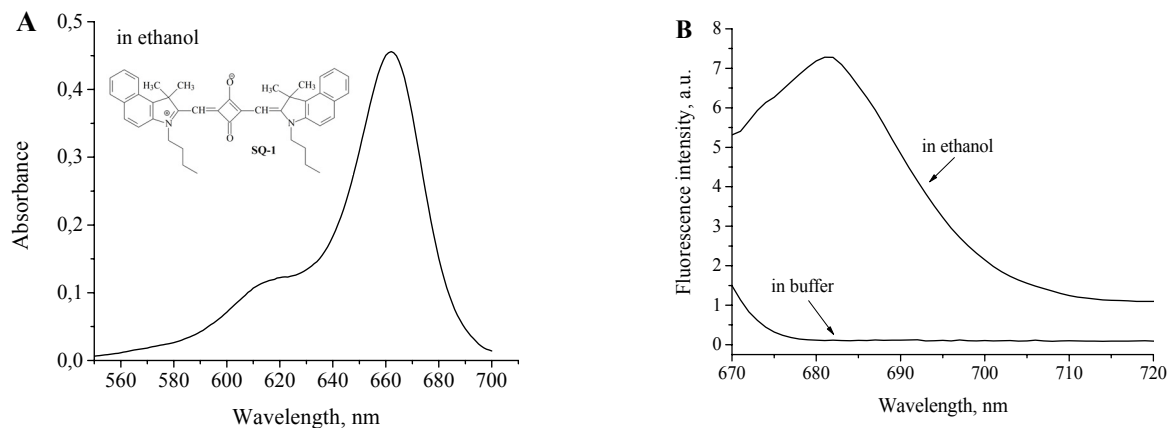


Fig. 1. SQ-1 absorption (A) and fluorescence (B) spectra
Shown in the inset is the chemical structure of SQ-1

To get further insights into the physicochemical properties of SQ-1 we performed the quantum-chemical calculations, which yielded the following molecular descriptors: a) descriptors of molecular geometry – CA , CV (cosmo area (solvent-accessible area) and cosmo volume (molecular volume), respectively), L , W , H (the length, width and height of the molecule, respectively), φ (dihedral angle of the molecule, or the angle of the rotation of central squarate moiety around the side groups of SQ-1), b) descriptors of electronic structure – $\sum Q(N)$, $\sum Q(C)$ (the sum of the charges on C and N atoms, respectively), E_{HOMO} , E_{LUMO} (the energies of the highest occupied and the lowest unoccupied molecular orbitals, respectively), μ_g , μ_e (the dipole moments of the ground and excited states, respectively), q_g , q_e (total charge on the donor group (side groups of SQ-1) in the ground and excited states, respectively), E_g , E_e (the energies of the ground and excited states), ΔE_e (the energy of vertical transition from the ground state to the lowest non-relaxed excited state, $S_0 \rightarrow S_1^{abs}$), f (the oscillator strength), c) descriptors of intermolecular interactions – $\log P$ (octanol/water partition coefficient), P (polarization of the molecule at electric field strength of 0 eV). The results of quantum-chemical calculations are given in Table 1.

The most interesting findings can be summarized as follows:

- the difference between E_{LUMO} and E_{HOMO} (the so-called HOMO/LUMO gap) is *ca.* 5.1 eV suggesting the high stability of SQ-1;
- the ground and excited state dipole moments have similar values. This finding correlates with the experimentally observed small Stokes shift and may underlie the insensitivity of SQ-1 spectral behavior to the effects of red-edge excitation shift;

- SQ-1 is characterized by small values of dihedral angle (*ca.* 12°) and height (2.9 Å) implying a high degree of planarity of the molecule;
- $\log P$ for SQ-1 is ~ 6 , pointing to a high lipophilicity of the dye. Thus, it might be expected that SQ-1 would display a strong affinity for lipid membranes. Indeed, as will be shown in the next section, our experimental results corroborate these theoretical predictions.

Table 1.

Quantum chemical characteristics of SQ-1

$CA, \text{Å}^2$	$CV, \text{Å}^3$	E_{HOMO}, eV	E_{LUMO}, eV	$\log P$	$\sum Q(N)$	$\sum Q(C)$	$L, \text{Å}$	$W, \text{Å}$	$H, \text{Å}$
605	780	-7.0	-1.9	6.08	-0.38	-5.38	17.0	9.4	2.9
$P, \text{Å}^3$	μ_g, D	μ_e, D	$E_g, \text{Hartree}$	f	$\Delta E_e, \text{cm}^{-1}$	$E_e, \text{Hartree}$	$\varphi, \text{deg.}$	q_g	q_e
87	2.09	2.09	-1885.751	1.201	17011	-1885.674	12	0.45	-0.12

SQ-1 binding to lipid membranes

The development of highly specific fluorescent probes for tracing the membrane-related processes still represents one of the major challenges in the membrane studies. One of the obstacles limiting the applicability of the available fluorophores lies in the overlap between the spectra of reporter molecules with those of the membrane components, especially proteins. Another problem stems from the requirement of high probe concentration in order to achieve the desirable response. However, being employed in a high concentration, the organic dye may affect the physicochemical properties of the lipid bilayer. In this regard, squaraine dyes seem to be extremely promising since: i) their spectral responses are not distorted by the background signals (i.e. light scattering, autoabsorption and autofluorescence); and ii) they have an excellent performance at low concentrations. Several successful membrane-specific squaraine fluorophores with attractive optical properties have been designed previously. Specifically, K1350, the novel squaraine derivative has been synthesized and identified as a probe sensitive to the changes in membrane polarity [19]. Next, three new amphiphilic squaraine dyes have been demonstrated to be suitable for fluorescence imaging of plasma membranes [29].

In the present study, we made an attempt to broaden the molecular library of existing membrane probes, representatives of squaraines, by evaluation the lipid-associating potential of SQ-1. To this end, the dye fluorescence spectra were recorded in liposome suspensions at varying lipid concentrations. As shown in Fig. 2, the SQ-1 partitioning into lipid bilayer is followed by a substantial enhancement of the dye fluorescence.

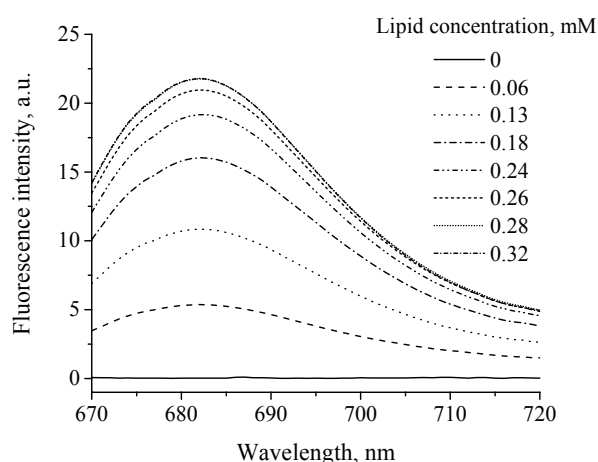


Fig. 2. Emission spectra of SQ-1 upon its binding to PC/CL (5 mol%) lipid vesicles. Probe concentration was 1.4 μM .

decrease in k_{nr} . The non-radiative deactivation is connected with the fluorophore rotational mobility, which, in turn, strongly depends on the nature of the probe surroundings [30]. The restrictions imposed by a lipid environment hinder the internal motion of SQ-1, decreasing the non-radiative decay rates and giving rise to the increase in the fluorescence quantum yield. Analysis of the chemical structure of SQ-1 allowed us to assume that zwitterionic in nature chromophore of this dye resides at the polar/nonpolar interface while butyl tails penetrate the hydrophobic bilayer

Importantly, the membrane-bound SQ-1 is featured by one-component fluorescence spectra indicating that the probe is in a monomeric form. According to our estimates, the quantum yield of SQ-1 reaches the value ~ 0.6 upon its association with the model lipid membranes. The rise in fluorophore emission is generally interpreted by the probe transfer to the medium with lower polarity and hindered rotation of the fluorophore. According to a classical definition, fluorescence quantum yield ϕ is given by:

$$\phi = \frac{k_r}{k_r + k_{nr}} \quad (2)$$

where k_r and k_{nr} are the rates of radiative and non-radiative relaxation processes, respectively [1].

It is assumed that k_r is independent of the probe environment, while the non-radiative decay processes are affected by the environmental conditions and the probe interactions with its surroundings. Therefore, the increase in fluorescence quantum yield can be attributed to the

region, being oriented parallel to the lipid acyl chains. In such a manner, the probe is immobilized within the membrane, which results in the inhibition of its rotation and the burst of fluorescence. Notably, modification of the physicochemical properties of lipid bilayers by inclusion of 2.5, 5 or 10 mol% of anionic lipid cardiolipin (CL) into phosphatidylcholine (PC) membranes led to insignificant change in SQ-1 fluorescence intensity (increase up to 10% at the highest employed lipid-to-dye molar ratio) suggesting that electrostatic interactions are not predominant in the dye-lipid binding.

To quantify SQ-1 association with liposomes, the dye partition coefficients (K_{PL}) have been determined for the different lipid systems. To this end, the experimental dependencies of SQ-1 fluorescence increase on lipid concentration were analyzed within the framework of partition model described in detail in [22]. As seen from Table 2, the recovered partition coefficients are rather high, pointing to a good affinity of SQ-1 for the lipid membranes.

Table 2.

Parameters of SQ-1 partitioning into lipid phase			
System	Partition coefficient	Molar fluorescence, M^{-1}	χ^2
PC	2030±325	$3.3 \times 10^7 \pm 510$	0.23
CL2.5	939±97	$7.5 \times 10^7 \pm 643$	0.57
CL5	1079±147	$6.4 \times 10^7 \pm 327$	1.21
CL10	1468±205	$3.7 \times 10^7 \pm 462$	0.74

Interestingly, the K_{PL} value estimated for PC membranes exceeds those derived for CL-containing bilayers, corroborating the idea that SQ-1 partitioning into lipid bilayer is driven by hydrophobic rather than electrostatic interactions. The obtained results suggest that SQ-1 represents a prospective near-infrared probe for tracing the processes occurring in biological membranes. The key advantages of this fluorophore include the exceptional brightness in lipid media, the high partition coefficients, the absence of J- or H-aggregation in a lipid phase. It should be noted at this point that recent studies of Zhang et al. opened up a new horizon in the studies of squaraine-lipid interactions [31]. Specifically, it was shown that squaraine-functionalized liposomes can serve as stable biocompatible nanoprobe for photoacoustic tomography and tumor imaging. The confinement of squaraines to the lipid vesicles increases the performance of these dyes and provides their target-specific delivery. In view of these findings and the results presented here, one may assume that liposomal forms of SQ-1 may be also used for *in vitro* visualization of tumors.

SQ-1 as a sensor for lipid peroxidation reactions

At the next stage of exploring the possibilities of using SQ-1 for tracing the processes occurring in biological media, we evaluated the potential of this probe as a sensor for lipid peroxidation (LPO). Lipid peroxidation is a degenerative process that affects the unsaturated membrane lipids under the conditions of oxidative stress. This process involves a chain of free radical reactions initiating the cascade of events that substantially compromise the stability of biological membranes, eventually resulting in the loss of cell functioning and cell death. A lot of markers have been developed to detect the lipid free radicals, the majority of which are based on fluorescein, rhodamine or phosphine derivatives [32-34]. However, there is still a need for new tracers with improved characteristics. In the present work we described the novel fluorimetric assay designed for identification of reactive oxygen species (ROS). Lipid free radicals were generated in the model protein-lipid systems containing heme-proteins – methemoglobin (metHb) and cytochrome *c* (cyt *c*), and lipid vesicles composed of zwitterionic lipid phosphatidylcholine (PC) and its mixtures with 5, 10 or 20 mol% of cardiolipin (CL). These proteins are well-known activators of lipid peroxidation through either the iron-triggered decomposition of lipid hydroperoxides, or Fenton-like reaction, implying the formation of hydroxyl radicals [35,36].

As shown in Fig. 3, association of metHb and cyt *c* with the lipid vesicles was followed by a dramatic decrease of SQ-1 fluorescence. Furthermore, the magnitude of this effect increased with i) the molar fraction of CL, and ii) the time of protein-lipid interactions. Interestingly, in the absence of liposomes fluorescence intensity of SQ-1 was found to increase at increasing concentration of proteins. To prove that the observed changes of SQ-1 fluorescence in the lipid environment are produced by the dye interactions with the protein-induced ROS, analogous kinetic measurements were conducted with the well-known free radical scavengers, butylated hydroxytoluene (BHT) and thiourea (TU). As expected, these antioxidants suppressed the effect of metHb and cyt *c* on SQ-1 fluorescence (Fig. 3). These findings corroborate the idea that SQ-1 decolorization is provoked by the products of lipid peroxidation. Additional evidence for this idea comes from the observation that activation of LPO by metal-catalyzed oxidation system $FeSO_4 +$ ascorbate (FA) also resulted in the time-dependent decrease in SQ-1 fluorescence intensity.

It is noteworthy in the present context that while interpreting the results described here, one should account for the ability of transition metals to quench the fluorescence of near-infrared dyes [37]. This effect originates from the formation of charge-transfer complex between the metal ion and the dye, which acts as a π -donor ligand. The formation of such a complex perturbs the chromophoric system of the probe, giving rise to the decrease in its fluorescence. To test this possibility, we evaluated the sensitivity of SQ-1 to lipid free radicals, generated by UV irradiation. It appeared that

squaraine dye was virtually non-fluorescent in UV-irradiated liposomes while the irradiation of SQ-1 ethanolic solution was followed by insignificant decrease in the probe emission. These observations suggest that reduction of SQ-1 fluorescence in irradiated membranes stems from the fluorophore interactions with UV-produced ROS. Hence, the revealed bleaching of SQ-1 in the protein-lipid systems cannot be attributed to direct quenching of the dye fluorescence by iron ions, and originates from SQ-1 interactions with LPO products.

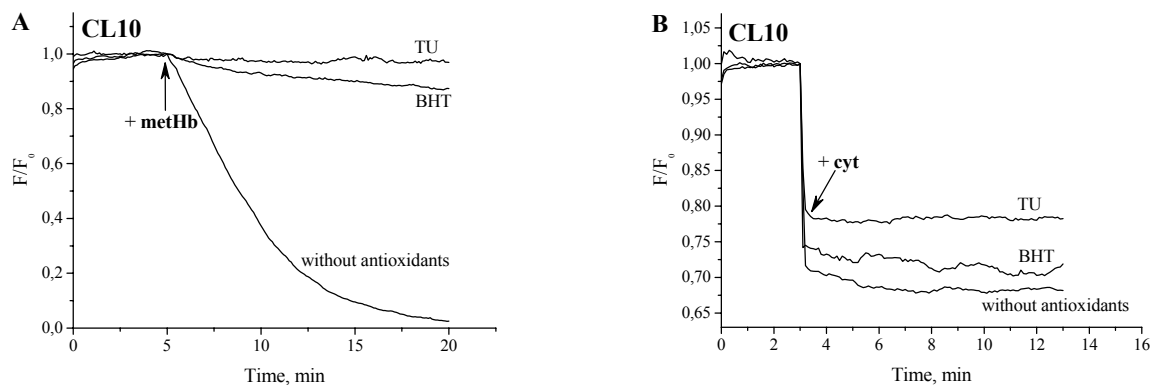


Fig.3. Time-dependent decrease in SQ-1 fluorescence

(A) upon the binding of methemoglobin, (B) cytochrome *c* to PC/CL (10 mol%) liposomes. The concentrations were: lipid – 0.08 mM, SQ-1 – 0.1 μ M, methemoglobin – 0.5 μ M, cytochrome *c* – 0.6 μ M

A question arises what molecular events underlie the decolorization of SQ-1? A vast majority of studies indicate that ROS may exert: i) direct influence on SQ-1 spectral properties via destruction of the probe structure; ii) indirect effect through the alterations in physicochemical properties of dye microenvironment brought about by the free radical-induced perturbations of the membrane structure; or iii) combination of both above cases. Considerable evidence suggests that direct attack of free radicals on the fluorescing compounds is accompanied by a pronounced decrease in fluorescence intensity. Several examples include the quenching of dipyridamole fluorescence by peroxy radicals [38], suppression of 1,3-diphenylisobenzofuran emission by superoxide anion radical [39], degradation of Alexa dye fluorescence by oxygen radicals [40], to name only a few. Giuvarch et al. classified the interactions of ROS species with fluorescent dyes into four main types: i) hydrogen atom abstraction; ii) electrophilic addition on a double bond; iii) oxidation of a double bond; and iv) electron transfer. Based on the results presented here, it seems impossible to identify unequivocally what type of interactions prevails in our systems. In an attempt to discover the structural features of SQ-1 which account for its sensitivity to free radicals, in a separate series of experiments we analyzed the potential of polymethine dye V2, structural analog of SQ-1 without the central squarate bridge, in detecting the lipid free radicals. It appeared that generation of ROS in liposomes by FA system resulted in 70%-decrease in SQ-1 fluorescence and only 30%-drop in V2 emission (data not shown). This finding suggests that the interactions between LPO products and SQ-1 occurs at the cyclobutene ring or in its vicinity. Apparently, free radical attack on the dye breaks down the C–C or C=C bonds adjoining to the central four-membered ring of SQ-1.

Along with this, increasing evidence indicates that lipid peroxidation can provoke profound changes in the structure and dynamics of lipid bilayer including [41-43]: i) increase in bilayer hydration and dielectric constant of a membrane core; ii) decrease in the density of acyl chain packing; iii) interdigitation of lipid tails; iv) rise in membrane viscosity due to cross-linking of free radicals. It cannot be excluded that these processes also contribute to the ROS-induced quenching of SQ-1 fluorescence. To summarize, the results presented in this section, strongly suggest that SQ-1 represents a prospective fluorescent reagent for detection of the reactive oxygen species, and can be used as a component of free radical sensing platforms.

SQ-1 as a probe for detection and structural characterization of amyloid fibrils

Excellent performance of SQ-1 in the lipid membrane studies allowed us to pose a question of whether this dye is suitable for protein characterization? A good deal of existing data show successful utilization of squaraines as covalent and noncovalent labels. To exemplify, the interaction of these dyes with bovine and human serum albumins was reported to be followed by: a) increase in fluorescence intensity; b) color change from orange to deep purple; and c) red shift in absorption spectra [44-46]. Based on these results, it was concluded that squaraines may serve as dual-mode recognition sensors for serum albumins. Red-shifted absorption, enhanced fluorescence and increased lifetime were also observed upon squaraine complexation with ovalbumin, and the conclusion has been drawn about the applicability of the fluorophores as contrast agents for *in vitro* and *in vivo* protein imaging [47]. In the current contribution, we assessed the sensitivity of SQ-1 to a special class of proteinaceous assemblies, amyloid fibrils. These structures represent highly ordered protein fibrillar aggregates composed of misfolded proteins and sharing a core cross- β -sheet structure [48].

Accumulation of amyloid fibrils in different tissues is currently regarded as a hallmark of a wide range of debilitating disorders, including Alzheimer's, Parkinson's diseases, type II diabetes, etc [49]. In view of this, timely detection of fibrillar aggregates is of paramount importance for prevention and inhibition of amyloid growth. A common strategy for the identification of amyloid fibrils is based on the use of specific fluorescent dye Thioflavin T [50]. However, this probe suffers from several drawbacks, associated with its sensitivity to the changes in environmental conditions (pH, ionic strength), the presence of exogenous compounds and the morphology of amyloid fibrils. These considerations highlight the necessity of the development of novel fluorescent markers for pathogenic protein aggregates. In this section, we evaluated the ability of SQ-1 to identify the amyloid structures. Specifically, our goal was two-fold: i) to estimate the parameters of the dye binding to fibrillar protein; and ii) to test the applicability of SQ-1 to structural characterization of amyloid fibrils. As a model protein we utilized hen egg white lysozyme which is highly prone to fibrillization *in vitro* under denaturing conditions.

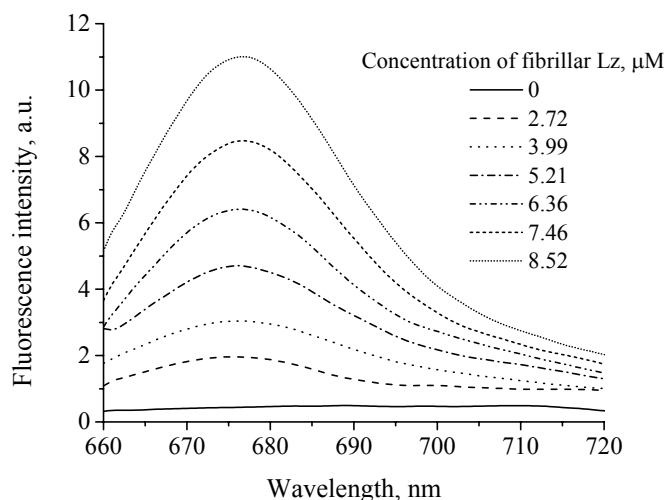


Fig.4. Fluorescence spectra of SQ-1 upon its association with lysozyme amyloid fibrils

is determined by peculiar fluorophore location within the fibril structure [50,51]. It has been proposed that amyloid-specific dyes, such as Thioflavin T, associate with fibrillar aggregates via insertion into the grooves formed between every other row of side chains, with the dye long axis being parallel to the fibril axis. This results in a significant restriction of the dye mobility, and, as a consequence, enhancement of its fluorescence by the orders of magnitude. The average width of such binding channel is about 6.5-6.9 Å [52]. This means that to be accommodated within the groove with the long axis parallel to fibril axis, the "thickness" of the dye molecule should not exceed the above values. As shown in Table 1, the "thickness" of SQ-1, defined as the height therein, is 2.9 Å, which fits the size of the amyloid groove. However, the dimensions of the probe are evaluated neglecting the length of its butyl tails. These hydrophobic chains are likely to hamper the incorporation of the dye molecule into the amyloid channel. Thus, we assumed that the most probable disposition of SQ-1 on the amyloid fibrils involves surface binding of the dye with its tails anchored in the fibril groove.

At the next step of the study the Förster resonance energy transfer (FRET) technique was employed to assess the possibilities of using SQ-1 in structural characterization of amyloid fibrils. Squaraine probes SQ-1 and V2, and aminobenzanthrone dye ABM were recruited as the components of the two donor-acceptor pairs – ABM-SQ-1 and SQ-1-V2. In both cases the addition of acceptor brought about the progressive decrease in donor fluorescence and appearance of the band of acceptor emission. The results of FRET experiments were treated in terms of the stretched exponential model [53]:

$$Q_r = \int_0^{\infty} \exp\left(-\lambda - C_A V_d \Gamma(1-d/6) \lambda^{d/6}\right) d\lambda, \quad (3)$$

where $\lambda = t/\tau_D$, τ_D is the donor fluorescence lifetime in the absence of acceptor; $V_d = \pi^{d/2} R_o^d / \Gamma\left(\frac{d}{2} + 1\right)$ is the volume of d -dimensional sphere of radius R_o , d is the dimensionality of fluorophore distribution (fractal dimension); $C_A = C_B / C_P V_{PF}$, C_P is the total protein concentration; V_{PF} is the volume of lysozyme molecule in a fibrillar state, C_B is the molar concentration of bound acceptor which was calculated from the results of binding studies.

Fig. 5, A represents the set of model parameters $\{V_{PF}, d\}$ which provides the best approximation of experimental data assuming that the donors and acceptors are freely rotating ($\kappa^2 = 0.67$). If this assumption is true, the $\{V_{PF}, d\}$

As seen in Fig. 4, the binding of SQ-1 to lysozyme fibrils is followed by the increase in the dye fluorescence intensity with the spectrum maximum around 677 nm, being suggestive of SQ-1 transfer to nonpolar environment. For quantitative analysis of the dye-protein association, the results of direct and inverse fluorimetric titrations were interpreted within the framework of Langmuir adsorption model [24]. Global fitting of the obtained data yielded the association constant and the number of binding sites, which were found to be $4.4 \pm 1.1 \mu\text{M}^{-1}$ and 0.25 ± 0.08 , respectively. Notably, Thioflavin T binding constant (*ca.* $0.04 \pm 0.01 \mu\text{M}^{-1}$, [24]) is two orders of magnitude lower than that of SQ-1, implying the higher affinity of squaraine dye to the fibrillar lysozyme in comparison with the classical amyloid marker. An increasing number of reports supports the notion that amyloid specificity of the dyes is

curves obtained for the two employed donor-acceptor pairs, would have a point of intersection, (V_{PF}^*, d^*) , defining the volume per lysozyme monomer and fractal dimension of the protein fibrils.

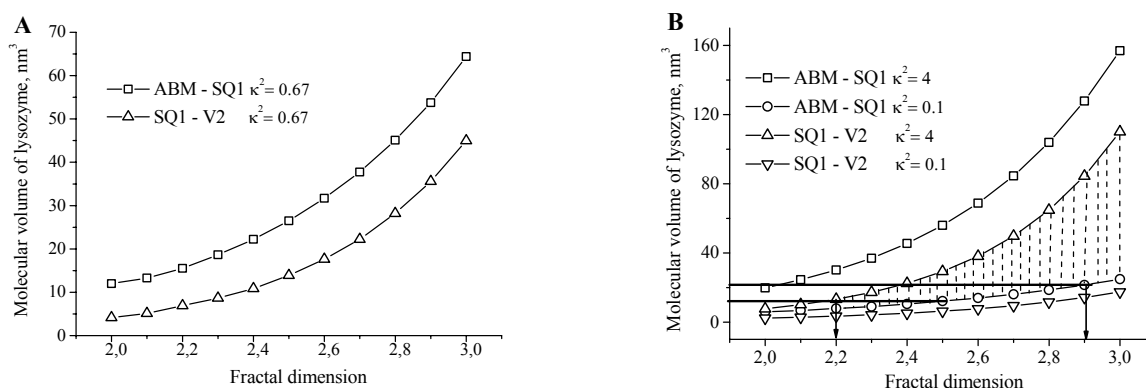


Fig.5. Dependencies of monomer molecular volume on fractal dimension of lysozyme amyloid fibrils calculated from Eq. (4) (A) at fixed, (B) varied values of orientation factor

However, as shown in Fig. 5, B the $V_{PF}(d)$ dependencies do not intersect, suggesting that the assumption about isotropic value of orientation factor is invalid since the rotation of donors and acceptors is restricted in a fibrillar environment. To overcome the problem of unknown orientation factor, in the following analysis κ^2 was varied within the possible limits which embrace all relative orientations of the donor and acceptor dipoles, from perpendicular ($\kappa^2 = 0$) to parallel ($\kappa^2 = 4$). The overlap between the regions which are limited by $V_{PF}(d)$ values, obtained for the two donor-acceptor pairs, yields the most probable $\{V_{PF}, d\}$ sets. It turned out that the volume of lysozyme monomer in a fibrillar state lies in a range 12-22 nm³, while fractal dimension of fibrillar protein varies from 2.2 to 2.9. Overall, the results outlined in this section, suggest that SQ-1 may be recommended as effective reporter molecule for spectroscopic detection and structural characterization of amyloid fibrils.

CONCLUDING REMARKS

Overall, the present contribution was intended to demonstrate the versatility of the novel squaraine probe SQ-1 as a prospective agent for a wide variety of bioapplications. This dye exhibits negligible fluorescence in aqueous solutions but shows considerable increase in emission upon conjugation with lipid bilayers, making it an ideal candidate for monitoring the processes occurring in biological membranes. Furthermore, fluorescence kinetic studies revealed the extremely high sensitivity of SQ-1 to the reactive oxygen species, opening the new horizons of squaraines' utilization in free radical sensing. Finally, SQ-1 showed excellent performance in the identification and structural characterization of the protein fibrillar aggregates suggesting its potential application in the design of fluorescence-based assays for early detection of amyloid fibrils and analysis of their microstructure. There is no doubt that potential uses of SQ-1 are not exhausted by the discussed possibilities and new proofs of squaraine versatility will appear soon. The most exciting future directions of SQ-1 use in biomedical research seem to involve: i) evaluating the potential of this probe in photodynamic therapy; ii) designing the reactive form of SQ-1 suitable for covalent protein labeling; iii) synthesis of SQ-1 derivatives with unique selectivity for different types of lipid free radicals.

REFERENCES

- Lakowicz J.R. Principles of fluorescent spectroscopy, 3rd edition. – New York: Springer, 2006.
- Natarajan A.T. Fluorescence in situ hybridization (FISH) in genetic toxicology // J. Environ. Pathol. Toxicol. Oncol. – 2001. – Vol. 20. – P. 293-298.
- Pruitt S.C., Melnicki L.M., Stewart C.C. Analysis of fluorescent protein expressing cells by flow cytometry // Methods Mol. Biol. – 2004. – Vol. 263. – P. 239-258.
- Leblond F., Davis S., Valdes P., Pogue B. Pre-clinical whole-body fluorescence imaging: review of instruments, methods and applications // J. Photochem. Photobiol. B. – 2010. – Vol. 98. – P. 77-94.
- Terai T., Nagano T., Small-molecule fluorophores and fluorescent probes for bioimaging // Pflugers Arch. – 2013. – Vol. 465. – P. 347-359.
- Willets K., Ostroverkhova O., He M., Twieg R., Merner W. Novel fluorophores for single-molecule imaging // J. Am. Chem. Soc. – 2013. – Vol. 125. – P. 1174-1175.
- Pansare V., Hejazi S., Faenza W., Prud'homme R. Review of long-wavelength optical and NIR imaging materials: contrast agents, fluorophores and multifunctional nano carriers // Chem. Mater. – 2012. – Vol. 24. – P. 812-827.
- Kim E., Lee Y., Lee S., Park S. Discovery, understanding and bioapplication of organic fluorophore: a case study with an indolizine-based novel fluorophore // Acc. Chem. Res. – 2015. – Vol. 48. – P. 538-547.

9. Ramaiah D., Eckert I., Arun K., Weidenfeller, Epe B. Squaraine dyes for photodynamic therapy: mechanism of cytotoxicity and DNA damage induced by halogenated squaraine dyes plus light (>600 nm) // *Photochem. Photobiol.* – 2004. – Vol. 79. – P. 99-104.
10. Qin C., Wong W., Han L. Squaraine for dye-sensitized solar cells: recent advances and future challenges // *Chem. Asian J.* – 2013. – Vol. 8. – P. 1706-1719.
11. Sleiman M., Ladame S. Synthesis of squaraine dyes under mild conditions: applications for labelling and sensing of biomolecules // *Chem. Commun.* – 2014. – Vol. 50. – P. 5288-5290.
12. Hu L., Yan Z., Hu H. Advances in synthesis and application of near-infrared absorbing squaraine dyes // *RSC Advances.* – 2013. – Vol. 3. – P. 7667-7676.
13. Law K., Bailey F. Squaraine chemistry: effect of synthesis on the morphological and xerographic properties of photoconductive squaraines // *J. Imag. Sci.* – 1987. – Vol. 31. – P. 172-175.
14. Merritt V., Hovel H. Organic solar cells of hydroxysquarylium // *Appl. Phys. Lett.* – 1976. – Vol. 29. – P. 414-416.
15. Shafeekh K., Rahim M., Basheer M., Suresh C., Das S. Highly selective and sensitive colourimetric detection of Hg²⁺ ions by unsymmetrical squaraine dyes // *Dyes and Pigments.* – 2013. – Vol. 96. – P. 714-721.
16. Wang W., Fu A., You J., Gao G., Lan J., Chen L. Squaraine-based colorimetric and fluorescent sensors for Cu²⁺-specific detection and fluorescence imaging in living cells // *Tetrahedron.* – 2010. – Vol. 66. – P. 3695-3701.
17. Ramaiah D., Eckert I., Arun K., Weidenfeller L., Epe B. Squaraine dyes for photodynamic therapy: study of their cytotoxicity and genotoxicity in bacteria and mammalian cells // *Photochem. Photobiol.* – 2002. – Vol. 76. – P. 672-677.
18. Xu Y., Li Z., Malkovskiy A., Sun S., Pang Y. Aggregation control of squaraines and their use as near-infrared fluorescent sensors for protein // *J. Phys. Chem. B.* – 2010. – Vol. 114. – P. 8574-8580.
19. Ioffe V., Gorbenko G., Domanov Ye., Tatars A., Patsenker L., Terpetschnig E., Dyubko T. A new fluorescent squaraine probe for the measurement of membrane polarity // *J. Fluoresc.* – 2006. – Vol. 16. – P. 47-52.
20. Ioffe V., Gorbenko G., Tatars A., Patsenker L., Terpetschnig E. Examining protein-lipid interactions in model systems with a new squarylium fluorescent dye // *J. Fluoresc.* – 2006. – Vol. 16. – P. 547-554.
21. Ahn H., Yao S., Wang X., Belfield K. Near-infrared-emitting squaraine dyes with high 2PA cross-sections for multiphoton fluorescence imaging // *ACS Appl. Mater. Interfaces.* – 2012. – Vol. 4. – P. 2847-2854.
22. Ioffe V., Gorbenko G., Deligeorgiev T., Gadjev N., Vasilev A. Fluorescence study of protein-lipid complexes with a new symmetric squarylium probe // *Biochem. Chem.* – 2007. – Vol. 128. – P. 75-86.
23. Trusova V., Gorbenko G., Deligeorgiev T., Gadjev N., Vasilev A. A novel squarylium dye for monitoring oxidative processes in lipid membranes // *J. Fluoresc.* – 2009. – Vol. 19. – P. 1017-1023.
24. Gorbenko G., Trusova V., Kirilova E., Kirilov G., Kalnina I., Vasilev A., Kaloyanova S., Deligeorgiev T. New fluorescent probes for detection and characterization of amyloid // *Chem. Phys. Lett.* – 2010. – Vol. 495. – P. 275-279.
25. Mui B., Chow L., Hope M. Extrusion technique to generate liposomes of defined size // *Meth. Enzymol.* – 2003. – Vol. 367. – P. 3-14.
26. Bartlett G. Phosphorus assay in column chromatography // *J. Biol. Chem.* – 1959. – Vol. 234. – P. 466-468.
27. Holley M., Eginton C., Schaefer D., Brown L. Characterization of amyloidogenesis of hen egg lysozyme in concentrated ethanol solution // *Biochem. Biophys. Res. Commun.* – 2008. – Vol. 373. – P. 164-168.
28. Oswald B., Lehmann F., Simon L., Terpetschnig E., Wolbeis O. Red laser-induced fluorescence energy transfer in an immunosystem // *Anal. Biochem.* – 2000. – Vol. 280. – P. 272-277.
29. Collot M., Kreder R., Tatars A., Patsenker L., Mely Y., Klymchenko A. Bright fluorogenic squaraines with tuned cell entry for selective imaging of plasma membrane vs. endoplasmic reticulum // *Chem. Commun.* – 2015. – Vol. 51. – P. 17136-17139.
30. Gaisenk V., Sarzhevsky A. Anisotropy of absorption and luminescence of polyatomic molecules, 1986.
31. Zhang D., Zhao Y., Qiao Y., Mayerhoffer U., Spent P., Li X., Wurthner F. Nano-confined squaraine dye assemblies: new photoacoustic and near-infrared fluorescence dual-modular imaging probes in vivo // *Bioconjug. Chem.* – 2014. – Vol. 25. – P. 2021-2029.
32. Hempel S., Buettner G., O'Malley Y., Wessels D., Flaherty D. Dihydrofluorescein diacetate is superior for detecting intracellular oxidants: comparison with 2',7'-dichlorodihydrofluorescein diacetate, 5(and 6)-carboxy-2',7'-dichlorodihydrofluorescein diacetate, and dihydrorhodamine 123 // *Free Radical Biol. Med.* - 1999. – Vol. 27. – P. 146-159.
33. Akasaka K. Development of phosphine reagents for fluorometric determination of lipid hydroperoxides // *Tohoku J. Agricul. Res.* – 1995. – Vol. 45. – P. 111-119.
34. Wolfbeis O., Durkop A., Wu M., Lin Z. A europium-ion-based luminescent sensing probe for hydrogen peroxide // *Angew. Chem.* – 2002. – Vol. 41. – P. 4495-4498.
35. Rogers M., Patel R., Reeder B., Sarti P., Wilson M., Alavash A. Pro-oxidant effects of cross-linked haemoglobins explored using liposome and cytochrome c oxidase vesicle model membranes // *Biochem. J.* – 1995. – V. 310. – P. 827-833.
36. Sadzadeh S., Graf E., Panter S., Hallaway P., Eaton J. Hemoglobin. A biologic Fenton reagent // *J. Biol. Chem.* – 1984. – Vol. 259. – P. 14354-14356.
37. Tarazi L., Narayanan N., Sowell J., Patonay G., Strekowski L. Investigation of the spectral properties of a squarylium near-infrared dye and its complexation with Fe(III) and Co(II) ions // *Spectrochim. Acta A.* – 2002. – Vol. 58. – P. 257-264.
38. Iuliano L., Piccheri C., Coppola I., Pratico D., Micheletta F., Violi F. Fluorescence quenching of dipyrindamole associated to peroxyl radical scavenging: a versatile probe to measure the chain breaking antioxidant activity of biomolecules // *Biochim. Biophys. Acta.* – 2000. – Vol. 1474. – P. 177-182.
39. Ohyashiki T., Nunomura M., Katoh T. Detection of superoxide anion radical in phospholipid liposomal membrane by fluorescence quenching method using 1,3-diphenylisobenzofuran // *Biochim. Biophys. Acta.* – 1999. – Vol. 142. – P. 131-139.
40. Choudhury F., Sabat G., Sussman M., Nishi Y., Shohet J. Fluorohore-based sensor for oxygen radicals in processing plasmas // *J. Vacuum Sci. Technol. A.* – 2015. – Vol. 33. – P. 061305.
41. Wong-ekkabut J., Xu Z., Triampo W., Tang I., Tieleman D., Monticelli L. Effect of lipid peroxidation on the properties of lipid bilayers: a molecular dynamics study // *Biophys. J.* – 2007. – Vol. 93. – P. 4225-4236.

42. Wratten M., Vanginkel G., Vantveld A., Bekker A., Vanfaasen E., Sevanian A. Structural and dynamic effects of oxidatively modified phospholipids in unsaturated lipid membranes // *Biochemistry*. – 1992. – Vol. 31. – P. 10901-10907.
43. Mason R., Walter M., Mason P. Effect of oxidative stress on membrane structure: small-angle X-ray diffraction analysis // *Free Radic. Biol. Med.* – 1997. – Vol. 23. – P. 419-425.
44. Xu Y., Malkovskiy A., Pang Y. Graphene binding-promoted fluorescence enhancement for bovin serum albumin recognition // *Chem. Commun.* – 2011. – Vol. 47. – P. 6662-6664.
45. Jisha V., Arun K., Hariharan M., Ramaiah D. Site-selective binding and dual mode recognition of serum albumin by a squaraine dye // *J. Am. Chem. Soc.* – 2006. – Vol. 128. – P. 6024-6025.
46. Jisha V., Arun K., Hariharan M., Ramaiah D. Site-selective interactions: squaraine dye – serum albumin complexes with enhanced fluorescence and triplet yields // *J. Phys. Chem. B.* – 2010. – Vol. 114. – P. 5912-5919.
47. Volkova K., Kovalska V., Tatarets A., Patsenker L., Kryvorotenko D., Yarmoluk S. Spectroscopic study of squaraines as protein-sensitive fluorescent dyes // *Dyes and Pigments*. – 2007. – Vol. 72. – P. 285-292.
48. Harrison R., Sharpe P., Singh Y., Fairlie D. Amyloid peptides and protein in review // *Rev. Physiol. Biochem. Pharmacol.* – 2007. – Vol. 159. – P. 1-77.
49. Chiti F., Dobson C. Protein misfolding, functional amyloid, and human disease // *Ann. Rev. Biochem.* – 2006. – Vol. 75. – P. 333-366.
50. Krebs M., Bromley E., Donald A. The binding of thioflavin T to amyloid fibrils: localization and implications // *J. Struct. Biol.* – 2005. – Vol. 149. – P. 30-37.
51. Groenning M. Binding mode of Thioflavin T and other molecular probes in the context of amyloid fibrils – current status // *J. Struct. Biol.* – 2010. – Vol. 3. – P. 1-18.
52. Tycko R. Solid state NMR studies of amyloid fibril structure // *Annu. Rev. Phys. Chem.* – 2011. – Vol. 62. – P. 279-299.
53. Drake J., Klafter J., Levitz P. Chemical and biological microstructures as probed by dynamic // *Science*. – 1991. – Vol. 251. – P. 1574-1579.